Random Waypoint Mobility Model in Cellular Networks

ESA HYYTIÄ* and JORMA VIRTAMO

Networking Laboratory, Helsinki University of Technology, Finland

Abstract. In this paper we study the so-called random waypoint (RWP) mobility model in the context of cellular networks. In the RWP model the nodes, i.e., mobile users, move along a zigzag path consisting of straight legs from one waypoint to the next. Each waypoint is assumed to be drawn from the uniform distribution over the given convex domain. In this paper we characterise the key performance measures, mean handover rate and mean sojourn time from the point of view of an arbitrary cell, as well as the mean handover rate in the network. To this end, we present an exact analytical formula for the mean arrival rate across an arbitrary curve. This result together with the pdf of the node location, allows us to compute all other interesting measures. The results are illustrated by several numerical examples. For instance, as a straightforward application of these results one can easily adjust the model parameters in a simulation so that the scenario matches well with, e.g., the measured sojourn times in a cell.

Keywords: random waypoint model, mobility modelling, cellular networks, handovers

1 Introduction

In this paper we study one of the most popular synthetic mobility models called the random waypoint model (RWP). In the RWP model a node (i.e., a mobile user) moves directly towards the next waypoint at a certain velocity v. Once the node reaches the waypoint the next waypoint is drawn randomly from the uniform distribution over $\mathcal{A}$. Similarly, the velocity for the next leg is drawn independently from a velocity distribution. Furthermore, it is possible to introduce "thinking times" when the node reaches each waypoint.

RWP model was originally proposed in [8] and has since then been studied actively, especially within the context of ad hoc networks. The spatial node distribution in the RWP model has been studied, e.g., in [4, 2, 10]. In [6] we have derived an analytical formula for the stationary node distribution in an arbitrary convex domain $\mathcal{A}$ in plane, and later, in [7] the analysis is extended to $\mathbb{R}^n$. Furthermore, the connectivity properties of ad hoc networks have been studied in [3, 9] (including the RWP model).

To our knowledge, the effects of the RWP model to cellular network models have been only briefly studied in [4], where the authors limit themselves to study a domain consisting of $\alpha \times \beta$ identical rectangles and are able to derive a brute force equation for the mean number of cell changes during a one transition (leg), which allows one to determine the mean cell change rate (handover rate) as well. In this paper we take a more general approach and consider a system of n nodes moving according to RWP model in an arbitrary convex domain $\mathcal{A} \subset \mathbb{R}^2$ which is divided into arbitrary pointwise disjoint partitions corresponding to, e.g., cells in a mobile cellular network. As

the nodes in the RWP model are assumed to move independently of each other we can consider a system with a single node without loss of generality. First we concentrate on the characterisation of the RWP process from the point of view of a given cell. The interesting quantities in this case are 1) the mean arrival (and departure) rate into cell j, denoted by $\lambda_j = 1/R_j$, where R_j is the mean time between two arrivals to cell j, and 2) the mean sojourn time in cell j, denoted by S_j, and its distribution ("service time").

More generally, one could be interested in the distributions of these quantities, but often the mean values are sufficient and in this paper we concentrate on those. Alternatively one can consider the system from the mobile node's point of view. As a corollary of the mean arrival rates into different cells one also obtains the mean handover rate in the network.

The rest of the paper is organized as follows. First, in Section 2 we formally describe the RWP process, make some remarks on its properties, and restate the main results of the earlier work. Then, in Section 3 the analytical formulæ for determining the mean arrival rates into an arbitrary cell are first derived. Then, results for some related measures and an extension to a RWP model with thinking times are presented and discussed. Section 4 contains some numerical examples and Section 5 the conclusions.

2 Random Waypoint Model

In the RWP model a node moves in a convex domain $\mathcal{A} \subset \mathbb{R}^2$ along a straight line segment from one waypoint to the other. The waypoints, denoted by P_i, are uniformly distributed in $\mathcal{A}$, $P_i \sim \mathrm{U}(\mathcal{A})$. Transition from P_{i-1} to P_i is referred to as the ith leg, and the velocity of the node on ith leg is given by random variable v_i, $v_i \sim v$. In particu-

lar, in the RWP model it is assumed that P_i's and v_i's are all independent. With this notation the RWP process (of a single node) is defined by an infinite sequence of triples,

$$\{(P_0, P_1, v_1), (P_1, P_2, v_2), \ldots\}.$$

First we note that in the RWP process the consecutive legs are not independent as they share a common waypoint. However, in many cases, as pointed out in [4], one can consider independent legs, i.e. the respective independent random point process (IRP),

$$\{(P_0, P_1, v_1), (P_2, P_3, v_3), \ldots\}.$$

Furthermore, we note that the RWP process is "time reversible" in the sense that any path along the waypoints $P_0, P_1, \ldots, P_n$ is equally likely to occur as the time reversed path, $P_n, P_{n-1}, \ldots, P_0$. A direct consequence of this is the fact that arrival rates across any line segment or border are equal in both directions. In other words, the average number of customers moving from cell i to cell j per time unit is equal to the number of customers moving from cell j to cell i per time unit (cf. a detailed balance in Markovian theory [11]). However, this process lacks the memoryless property of Markov chains, because, e.g., it is obvious that due to the used mobility model a node arriving from a certain cell is more likely to continue in the same direction and depart the cell at the opposite border of the cell.

2.1 Node Distribution in RWP Model

Next let us recap the main results from [6]. Let $a_1 = a_1(\mathbf{r}, \phi)$ denote the distance from point $\mathbf{r} \in \mathcal{A}$ to the border of $\mathcal{A}$ in direction ϕ. Similarly, let a_2 denote the distance to the border in opposite direction, i.e., $a_2(\mathbf{r}, \phi) = a_1(\mathbf{r}, \phi + \pi)$. Define[1]

$$h(\mathbf{r}, \phi) = \frac{1}{2} \cdot a_1 a_2 (a_1 + a_2).$$

The stationary distribution of a node moving according to RWP model is given by (see [6])

$$f(\mathbf{r}) = \frac{1}{C} \int_0^{2\pi} h(\mathbf{r}, \phi) \, d\phi, \qquad (1)$$

where parameter C is the normalisation constant,

$$C = \overline{\ell} A^2, \qquad (2)$$

where $\overline{\ell}$ is the mean length of leg and A the area of the domain $\mathcal{A}$. Hence, the mean leg length can be obtained by normalisation,

$$\overline{\ell} = \frac{1}{A^2} \int_{\mathcal{A}} \int_0^{2\pi} h(\mathbf{r}, \phi) \, d\phi \, dA.$$

[1] Note that $h(\mathbf{r}, \phi)$ is symmetric with respect to ϕ, i.e., $h(\mathbf{r}, \phi) = h(\mathbf{r}, \phi + \pi)$.

The values of the important constants related to the RWP model for some regular domains (unit disk, unit box and hexagon) are presented in Table 1.

Example: For a unit disk Eq. (1) reduces into (see [6])

$$f(r) = \frac{h(r)}{C} = \frac{45(1 - r^2)}{64\,\pi} \int_0^{\pi} \sqrt{1 - r^2 \cos^2 \phi} \, d\phi,$$

where $C = 128\pi/45$, and

$$h(r) = \frac{(1 - r^2)}{2} \int_0^{\pi} \sqrt{1 - r^2 \cos^2 \phi} \, d\phi.$$

Especially, at $r = 0$ we get

$$f(0) = \frac{45}{64} \quad \text{and} \quad h(0) = \frac{\pi}{2}. \qquad (3)$$

2.2 Mean Transition Times

In the basic form of the RWP process the velocity of the node is assumed to be a constant $v = 1$ on all legs, in which case the mean transition time is clearly equal to the mean length of leg. In a more general form we have a velocity distribution, denoted by $f_v(v)$, from which we draw a velocity for each leg independently. In other words, on each leg i the node travels on a constant velocity v_i, which is drawn from the velocity distribution $f_v(v)$ at the start of the ith leg. Letting T_i denote the transition time on ith leg we have

$$T_i = \frac{\ell_i}{v_i}, \qquad \text{where } \ell_i = |P_i - P_{i-1}|,$$

where ℓ_i and v_i are independent random variables. Hence, the mean transition time, i.e., the time from one waypoint to another, is given by [1, 6]

$$\mathrm{E}[T] = \overline{\ell} \cdot \int_v \frac{1}{v} f_v(v) \, dv = \overline{\ell} \cdot \mathrm{E}[1/v], \qquad (4)$$

while the quantity

$$f_v^{(*)}(v) = \frac{1}{\mathrm{E}[1/v]} \cdot \frac{1}{v} \cdot f_v(v),$$

corresponds to the probability distribution of the node's velocity at an arbitrary point of time. In the rest of the paper we assume that

$$\mathrm{E}[1/v] < \infty, \qquad (5)$$

as otherwise all the nodes eventually stop moving (see [14, 1, 6]). A typical choice for the velocity distribution is the uniform distribution from $v_{\min}$ to $v_{\max}$, which yields

$$\mathrm{E}[T] = \frac{\overline{\ell} \cdot \ln(v_{\max}/v_{\min})}{v_{\max} - v_{\min}},$$

where we assume that $v_{\min} > 0$ in order to have a finite $\mathrm{E}[1/v]$ in accordance with Eq. (5).

domain	$\overline{\ell}$		A		$C = \overline{\ell} \cdot A^2$	
unit disk	$128/(45\pi)$	≈ 0.905	π	≈ 3.142	$128\pi/45$	≈ 8.936
unit square		≈ 0.521	1			≈ 0.521
hexagon		≈ 0.83	$3\sqrt{3}/2$	≈ 2.598		≈ 5.58

Table 1: Parameters of the RWP model in some symmetrical domains [6].

3 Analysis of the System

We assume that the domain $\mathcal{A}$ is partitioned into n sub-domains, $\mathcal{A}_j$, $j = 1, \ldots, n$. Each $\mathcal{A}_j$ corresponds to cell j. Without loss of generality we consider a system with a single user. The results for a system with m independent and identically moving users are straightforward to obtain from the single user results.

3.1 Handover Rates

As mentioned already, our first aim is to determine the mean handover rates (or arrival rates). To this end, let λ_{ij} denote the handover rate from cell i to cell j, i.e., the average number of times a node moves from cell i to cell j per unit time. Consequently, the total handover rate (or arrival rate) into cell j, denoted by λ_j, is given by

$$\lambda_j = \sum_i \lambda_{ij}.$$

From the mobile node's point of view the interesting quantities are, e.g., the mean handover rate (in the network) and the expected number of times a mobile node has to make a handover during a typical call. In our case the mean handover rate in the network is easy to obtain, as it is simply the sum of the arrival rates into different cells,

$$\lambda_{\text{tot}} = \sum_{j=1}^{n} \lambda_j, \tag{6}$$

and the mean number of handovers during a call is $\lambda_{\text{tot}} \cdot T$, where T denotes the duration of the call.

Note that for a system with $m > 1$ users the arrival rates into cells are simply m times the respective arrival rate in a single user system. The handover rate from the mobile node's perspective naturally remains unchanged.

Furthermore, let random variable H denote the number of handovers occurring within a single leg. For the mean $\mathrm{E}[H]$ we have an elementary relationship [1]

$$\lambda_{\text{tot}} = \frac{\mathrm{E}[H]}{\mathrm{E}[T]} \quad \Rightarrow \quad \mathrm{E}[H] = C_v \cdot \lambda_{\text{tot}}/A^2, \tag{7}$$

where

$$C_v = C \cdot \mathrm{E}[1/v] = \overline{\ell} A^2 \cdot \mathrm{E}[1/v]. \tag{8}$$

Note that, unlike the handover rates (λ's), the number of handovers within a single leg, denoted by H, is independent of the velocity distribution (term C_v appears also in the denominator of λ_{tot}).
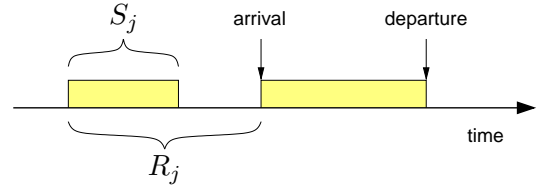

Figure 1: One arrival cycle: S_j is the mean sojourn time in cell j and R_j the mean time between two consecutive arrivals to cell j. Thus, the propability of finding a node in cell j is $p_j = S_j/R_j = \lambda_j \cdot S_j$ (cf. Little's result).

3.2 Mean Sojourn Time

One interarrival cycle to cell j is illustrated in Fig. 1. Let p_j denote the probability of finding a node in cell j. From Fig. 1 we obtain an elementary relation,

$$p_j = S_j/R_j = \lambda_j \cdot S_j, \tag{9}$$

i.e., Little's result for a system with one customer [5, 13]. Thus, it is enough to know any two unknowns in (9) and the third one can be easily determined. Using the results from [6, 7] we can easily compute p_j's and thus we need to find a way to compute either the mean sojourn time S_j or the mean time between two consecutive arrivals $R_j = 1/\lambda_j$. In this paper we present a general analytical formula for evaluating λ_{ij}'s and λ_j, which then allows us to compute S_j as well.

3.3 Mean Flow Across a Curve

From (1) one can identify that the quantity

$$\psi(\mathbf{r}, \phi) = \frac{h(\mathbf{r}, \phi)}{\mathrm{E}[1/v] \cdot C} = \frac{h(\mathbf{r}, \phi)}{C_v},$$

is the specific flux at point $\mathbf{r}$ in direction ϕ, i.e., the expected rate of crossings across a differential line segment perpendicular to direction ϕ per unit length of the segment and per unit angle. Note that if the velocity of the node is a constant, $v = 1$, from (8) we get $C_v = C$. Denote

$$\lambda(\mathbf{r}, \theta) = \int_0^\pi \sin\phi \cdot \psi(\mathbf{r}, \theta + \phi) \, d\phi$$

$$= \frac{1}{C_v} \int_0^\pi \sin\phi \cdot h(\mathbf{r}, \theta + \phi) \, d\phi,$$

which is the flux per unit length across a differential line segment at $\mathbf{r}$ pointing to the direction θ. Consequently,
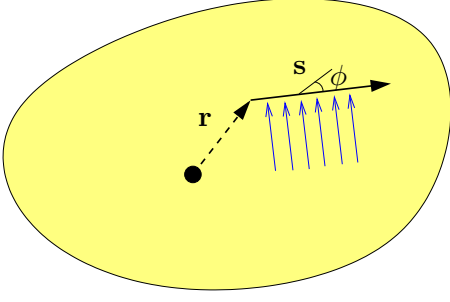
3

Figure 2: Consider transitions across vector s in figure.

the total flux crossing a given curve $\mathcal{C}$ from one side to the other is given by

$$\lambda(\mathcal{C}) = \int_{\mathcal{C}} \lambda(\mathbf{r}, \theta(d\mathbf{r})) \, dr, \qquad (10)$$

where $\theta(d\mathbf{r})$ is the direction of the tangent at point $\mathbf{r}$. In particular, when $\mathcal{C}$ is a closed curve, the total flux from outside to inside is given by the contour integral

$$\lambda(\mathcal{C}) = \oint_{\mathcal{C}} \lambda(\mathbf{r}, \theta(d\mathbf{r})) \, dr, \qquad (11)$$

where the integral is taken in the anti-clockwise direction.

Consider next a line segment $\mathcal{S}$ from point $\mathbf{r}$ to point $\mathbf{r} + \mathbf{s}$ as depicted in Fig. 2. Denote by $\mathbf{u}_s$ the unit vector along $\mathbf{s}$,

$$\mathbf{u}_s = \frac{\mathbf{s}}{|\mathbf{s}|} = (\cos\theta, \, \sin\theta).$$

From Eq. (10) one obtains that in this case the flux, i.e., the mean rate of transitions, across the line segment $\mathcal{S} = (\mathbf{r}, \mathbf{r} + \mathbf{s})$ in one direction is given by

$$\lambda(\mathcal{S}) = \frac{1}{C_v} \int_0^\pi \sin\phi \int_0^{|\mathbf{s}|} h(\mathbf{r} + t\mathbf{u}_s, \theta + \phi) \, dt \, d\phi. \qquad (12)$$

Thus, using one of Eqs. (10)-(12) we can compute the mean arrival rate into a cell. Consequently, together with Eqs. (1) and (9), we are also able to determine the mean sojourn time in the cell, $S_j = p_j/\lambda_j$. Note that if one is only interested in the mean sojourn time then the normalisation constant C is cancelled, i.e.,

$$S_j = \frac{\mathrm{E}\left[1/v\right] \int_{\mathcal{A}_j} \int_0^{2\pi} h(\mathbf{r}, \phi) \, d\phi \, dA}{\int_{\partial\mathcal{A}_j} \int_0^\pi \sin\phi \cdot h(\mathbf{r}, \theta(d\mathbf{r}) + \phi) \, d\phi \, dr},$$

where $\partial\mathcal{A}_j$ is the boundary of $\mathcal{A}_j$. Thus, the mean sojourn time in a cell is directly proportional to $\mathrm{E}\left[1/v\right]$.

3.4   Mean Flow Across a Straight Cut

In the previous section we presented general expressions for the arrival rate across a given boundary. In this section we focus our attention to a special case where the cells are formed by straight cuts across the area. Consequently, the cells themselves will be convex areas. First we make the observation that new legs are generated uniformly at the rate

$$\frac{1}{\mathrm{E}\left[T\right] \cdot A} = \frac{1}{\overline{\ell} \cdot \mathrm{E}\left[1/v\right] \cdot A} = \frac{A}{C_v}$$

per unit time and per unit area. This observation gives us an alternative way to determine the total flux into a convex cell $\mathcal{A}_j$. In particular, by conditioning on the turning points being outside $\mathcal{A}_j$ we get (IRP)

$$\lambda_j = \frac{1}{C_v} \int_{\mathcal{A}\backslash\mathcal{A}_j} B_j(\mathbf{r}) \, d^2\mathbf{r}, \qquad (13)$$

where $B_j(\mathbf{r})$ represents the area of the set of suitable destination points $\mathcal{B}_j(\mathbf{r})$,

$$\mathcal{B}_j(\mathbf{r}) = \{\mathbf{r}' \in \mathcal{A} \, : \, \ell(\mathbf{r}, \mathbf{r}') \cap \mathcal{A}_j \neq \emptyset\},$$

i.e., the set of such points $\mathbf{r}'$ that the line segment $\mathbf{r} \to \mathbf{r}'$ crosses the cell $\mathcal{A}_j$.

If $\mathcal{A}_j$ is a convex set separated from $\mathcal{A}$ by a straight line, then Eq. (13) can be further simplified since then the integrand is constant, $B_j(\mathbf{r}) = A_j$ for all $\mathbf{r} \in \mathcal{A} \setminus \mathcal{A}_j$, and consequently,

$$\lambda_j = \frac{A_j(A - A_j)}{C_v} = \frac{A_j/A(1 - A_j/A)}{\overline{\ell} \cdot \mathrm{E}\left[1/v\right]}. \qquad (14)$$

In other words, the flux across any cut obtained by a straight line is a function of the areas, and the product of the mean leg length and $\mathrm{E}\left[1/v\right]$ corresponding to the mean transition time according to (4). Note that it is straightforward to generalise this formula to $\mathbb{R}^n$, i.e., to the case where nodes move according to RWP model in a convex subset of $\mathbb{R}^n$ (see [7]).

Let us consider next an arbitrary convex domain $\mathcal{A}$, which has been divided into n partitions by m straight cuts. Each cut j splits the domain into two domains with areas A_j and $A - A_j$. Note that in this case $\mathcal{A}_i \cap \mathcal{A}_j$ is not necessarily an empty set. The mean arrival rate across cut j, in both directions, is given by Eq. (14),

$$\lambda_j^{(2)} = 2 \cdot \frac{A_j(A - A_j)}{C_v},$$

and hence the mean handover rate in the whole cellular network is given by

$$\lambda_{\mathrm{tot}} = \frac{2}{C_v} \sum_{j=1}^m A_j(A - A_j). \qquad (15)$$

4

Consequently, the mean number of handovers per transition, denoted by $\mathrm{E}\,[H]$, is given by

$$\mathrm{E}\,[H] = \lambda_{\text{tot}} \cdot \mathrm{E}\,[T] = \frac{2}{A^2} \sum_{j=1}^{m} A_j(A - A_j), \quad (16)$$

which is, obviously, independent of the velocity distribution. We emphasize that Eq. (16) holds for an arbitrary convex domain $\mathcal{A}$ which has been divided into cells by m arbitrary straight cuts.

3.5 Thinking Times

One popular extension to the standard RWP model is to add so-called thinking times at the turning points, i.e., upon reaching a waypoint the node waits a certain random time interval before taking a new direction towards the next waypoint. Assume that the thinking times are i.i.d. random variables, $\tau_i \sim \tau$, with mean $\overline{\tau}$. Formally, the RWP process is now defined by the infinite sequence of quadruples,

$$\{(P_0,\, P_1,\, v_1,\, \tau_1),\, (P_1,\, P_2,\, v_2,\, \tau_2),\, \ldots\}.$$

Let P_m denote the proportion of the time the node is moving, and similarly, let P_s denote the proportion of the time the node is still. As the lengths of the movement and the stopping periods are independent and the periods alternate we have, [12, 1, 6]

$$P_m = \frac{\overline{\ell} \cdot \mathrm{E}\,[1/v]}{\overline{\ell} \cdot \mathrm{E}\,[1/v] + \overline{\tau}} \quad \text{and} \quad P_s = \frac{\overline{\tau}}{\overline{\ell} \cdot \mathrm{E}\,[1/v] + \overline{\tau}}.$$

Let p_j^* and p_j denote the probabilities that a node is inside cell j in a model with and without thinking times, respectively. Then,

$$p_j^* = P_m \cdot p_j + P_s \cdot \frac{A_j}{A}.$$

A similar relation holds for the arrival rates. Let λ_j denote the mean arrival rate into cell j without thinking times, and λ_j^* the mean arrival rate with thinking times. Then it is easy to see that,

$$\lambda_j^* = P_m \cdot \lambda_j.$$

The mean sojourn time in a cell again follows from Little's result, i.e.,

$$S_j^* = \frac{p_j^*}{\lambda_j^*} = \frac{P_m \cdot p_j + P_s \cdot A_j/A}{P_m \cdot \lambda_j}$$
$$= S_j + \frac{A_j}{\overline{\ell} \cdot \mathrm{E}\,[1/v] \cdot A \cdot \lambda_j} \cdot \overline{\tau},$$

from which we can identify a quantity corresponding to the mean number of turns a node takes during a visit in

cell j, which is clearly independent of the possible thinking times. Accordingly, denoting this quantity by $N_j^{(T)}$, we have

$$\mathrm{E}\,\left[N_j^{(T)}\right] = \frac{A_j}{\overline{\ell} \cdot \mathrm{E}\,[1/v] \cdot A \cdot \lambda_j} = \frac{A_j \cdot A}{C_v \cdot \lambda_j}. \quad (17)$$

Note that this quantity includes also such visits where the node takes no turns inside the cell.

3.6 Convex Cells and Number of Turns

Let us next limit ourselves to case where a particular cell $\mathcal{A}_j \subset \mathcal{A}$ is convex. Then, on condition that the node makes at least one turn, the number of consecutive turns inside the convex cell $\mathcal{A}_j$ is geometrically distributed,

$$\mathrm{P}\{N_j^{(T)} = i | N_j^{(T)} > 0\} = (A_j/A)^{i-1} \cdot (1 - A_j/A),$$

and consequently,

$$\mathrm{E}\,\left[N_j^{(T)} | N_j^{(T)} > 0\right] = \frac{A}{A - A_j}.$$

Also we have

$$\mathrm{E}\,\left[N_j^{(T)}\right] = \mathrm{P}\{N_j^{(T)} > 0\} \cdot \mathrm{E}\,\left[N_j^{(T)} | N_j^{(T)} > 0\right]$$
$$+ \mathrm{P}\{N_j^{(T)} = 0\} \cdot 0.$$

By combining the last two equations with Eq. (17), we obtain a formula for the probability that an arriving node has the next waypoint within the (convex) cell $\mathcal{A}_j$,

$$\mathrm{P}\{N_j^{(T)} > 0\} = \frac{A_j(A - A_j)}{C_v \cdot \lambda_j}.$$

In particular, if $\mathcal{A}_j$ and $\mathcal{A} \setminus \mathcal{A}_j$ are both convex whence Eq. (14) holds and one obtains $\mathrm{P}\{N_j^{(T)} > 0\} = 1$. (This fact could have been easily deduced as well.)

By combining the above equations we finally get,

$$\mathrm{P}\{N_j^{(T)} = i\} =$$
$$\begin{cases} 1 - p_0, & \text{when } i = 0, \\ p_0 \cdot p^{i-1} \cdot (1 - p), & \text{when } i > 0, \end{cases} \quad (18)$$

where $p_0 = \mathrm{P}\{N_j^{(T)} > 0\}$ and $p = A_j/A$.

Using the above we can also derive an estimate for the asymptotic behaviour of the sojourn time S_j. Namely, for a large enough t we have

$$\mathrm{P}\{S_j > t\} \approx \mathrm{P}\{N_j^{(T)} \geq \frac{t}{\overline{\ell} \cdot \mathrm{E}\,[1/v]}\},$$

from what we deduce that

$$\mathrm{P}\{S_j > t\} \approx \mathrm{P}\{N_j^{(T)} > 0\} \cdot \left(\frac{A_j}{A}\right)^{\frac{t}{\overline{\ell} \cdot \mathrm{E}[1/v]} - 1},$$
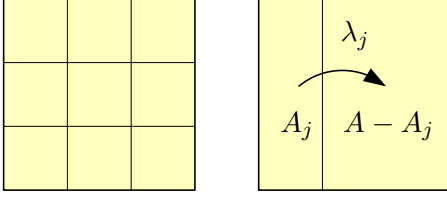
5

Figure 3: The handovers in 3×3 grid occur across 4 identical cuts, each of which separates the unit square into two domains with areas $1/3$ and $2/3$ (right fig.)

when $t \gg 1$. In other words, the tail distribution of the sojourn time S_j decreases approximately exponentially for $t \gg 1$,

$$P\{S_j > t\} \approx D \cdot e^{-\alpha t},$$

where

$$\begin{cases} D & = & (A/A_j) \cdot P\{N_j^{(T)} > 0\}, \\ \alpha & = & \dfrac{\ln(A/A_j)}{\overline{\ell} \cdot E\,[1/v]}. \end{cases}$$

3.7 Scaling the Domain and the Mean Velocity

Assume that the original domain $\mathcal{A}$ is scaled by a factor $q > 0$ in order to obtain a new domain $\mathcal{A}^*$. Furthermore, the velocity in the new domain is set to $\overline{v}^*$ instead of constant 1. In other words, the node location at time t is given by

$$\mathbf{r}^*(t) = q \cdot \mathbf{r}(\overline{v^*} \cdot t),$$

where $\mathbf{r}(t)$ is the node location in the original "mathematical model" and $\mathbf{r}^*(t)$ the node location in "real life scenario". Then, the following relations between the key performance figures hold:

$$\begin{array}{ll} p_j^* & = p_j, \\ S_j^* & = q\,/\,\overline{v^*} \cdot S_j, \\ \lambda_j^* & = \overline{v^*}\,/\,q \cdot \lambda_j. \end{array} \qquad (19)$$

4 Numerical Examples

4.1 Regular Grid Cells in Unit Square

Our first example is similar to the one considered by Bettstetter et al. in [1], where they consider a rectangular area divided into $\alpha \times \beta$ identical rectangular cells. The authors first present a brute force method for computing the mean number of cell changes (i.e., handovers) per transition by considering so-called Manhattan distance between each pair of cells, and then compute the mean cell change rate (handover rate) using the relation Eq. (7).

However, even a more general case can be easily solved by using Eq. (16).

Example 1: For a regular 3×3 grid the partitioning consists of 4 identical cuts with $A_j = 1/3$ and $(A - A_j) =$ 2/3, as depicted in Fig. 3. Substituting these into Eq. (16) gives us the mean number of handovers per transition,

$$E\,[H] = 8 \cdot (1/3) \cdot (2/3) = \frac{16}{9},$$

which matches with the result obtained in [1] by rather tedious numerical calculations.

Example 2: Similarly, it is straightforward to show that for an arbitrary $n \times m$ grid consisting of identical rectangular cells the mean number of handovers per transition is given by

$$E\,[H] = \frac{n(m^2 - 1) + m(n^2 - 1)}{3nm}, \qquad (20)$$

which can also be written as

$$E\,[H] = \frac{n + m}{3} - \frac{1/m + 1/n}{3},$$

in order to show the asymptotic behaviour.[2]

For the symmetric case $n = m$ Eq. (20) reduces into

$$E\,[H] = \frac{2(n^2 - 1)}{3n},$$

for which we have the obvious estimate,

$$E\,[H] \approx 2n/3, \quad \text{for } n \gg 1.$$

Furthermore, combining this with Eq. (7) gives us an estimate for the handover rate in a unit square divided into $n \times n$ cells,

$$\lambda_{\text{tot}} \approx \frac{1.28 \cdot n}{E\,[1/v]}, \quad \text{for } n \gg 1.$$

4.2 Regular Cells in Unit Square

Three possible example applications of Eq. (14) are illustrated in Fig. 4. In all cases, the flows across the shaded area and each of the white areas can be calculated using Eq. (14), and consequently the total arrival rate into the shaded cell can be determined as a sum of the arrival rates across each border. Hence, with little effort one obtains

$$a) \quad \lambda(h) = \frac{1}{C_v} \cdot h^2(2 - h^2), \qquad 0 \le h \le 1/2,$$

$$b) \quad \lambda(h) = \frac{1}{C_v} \cdot 2h(1 - h), \qquad 0 \le h \le 1/2,$$

$$c) \quad \lambda(h) = \frac{1}{C_v} \cdot \frac{3 + 6h - 9h^2}{8}, \qquad 0 \le h \le 1.$$

In Fig. 5 the resulting arrival rates are depicted as a function of parameter h. In cases (a) and (b) the resulting arrival rate increases monotonically as h increases from 0 to $1/2$. In case (c) the arrival rate first increases and reaches the maximum at point $h = 1/3$, and then decreases to zero as $h \to 1$. Nonetheless, parameter h is easy to adjust in all cases so that a desired arrival rate into the shaded cell is attained.

---

[2]This asymptotic behaviour is also discovered in [1] without an exact expression for the error term, $\epsilon = \frac{1/m + 1/n}{3}$.
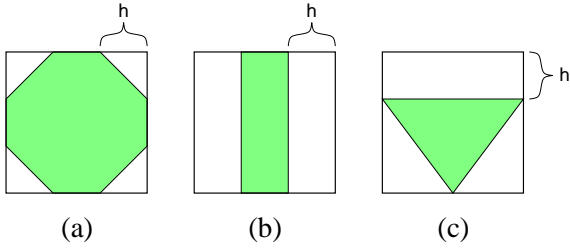
Figure 4: Three symmetric examples in unit square where the arrival rate into the cell is easy to determine using Eq. (14).
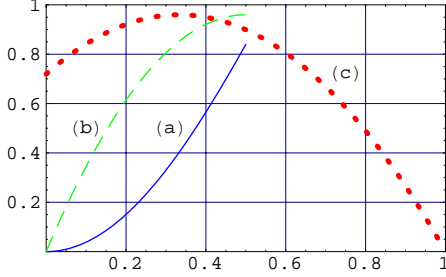

Figure 5: Resulting arrival rate into center cells of Fig. 4 examples as a function of parameter h. The solid curve corresponds to case (a), the long dashed curve to case (b) and the dotted curve to case (c).

4.3 Unit Disk: sector cell

In order to verify our results let us next consider a simple example of a unit disk which is split into two areas along the x-axis, i.e., the upper and the lower half disks. Let $\mathbf{r} = (-t, 0)$ as depicted in Fig. 6. Then, the distance to the border in direction ϕ is

$$a_1(t, \phi) = t \cos \phi + \sqrt{1 - t^2 \sin^2 \phi}.$$

For now assume that the node moves at the constant velocity of $v = 1$. Then, for instance the mean arrival rate to the upper half disk is given by

$$\lambda = \frac{2}{\bar{\ell}\pi^2} \int\limits_0^1 \int\limits_0^\pi \sin \phi \cdot h(t, \phi) \, d\phi \, dt,$$

where we have utilised the symmetry. From Table 1 we obtain that the mean length of leg in a unit disk is $\bar{\ell} = 128/(45\pi) \approx 0.905$, and hence the mean arrival rate can be determined by evaluating the integral. Numerically we obtain the mean arrival rate of 0.276.

On the other hand, this symmetric case can also be determined using Eq. (14),

$$\lambda = \frac{(\pi/2)^2}{C_v} = \frac{1}{4\bar{\ell}} = \frac{45\pi}{512} \approx \underline{0.276}.$$

Note that the flux in one direction across a radius of the disk is $\lambda/2$. Therefore, the flux inside an arbitrary sector of the unit disk is again λ. In particular, let the partitioning
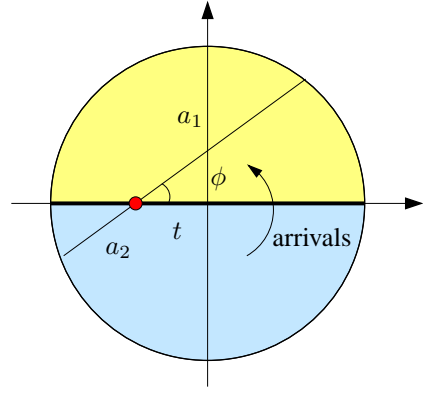

Figure 6: Transitions in unit disk from the lower half to the upper correspond to arriving customers.

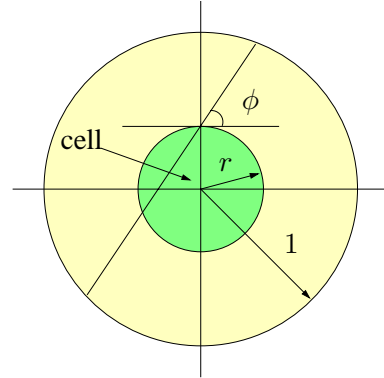Figure 7: Concentric circular cell inside a unit disk.

be given by a set of central angles, $\{\phi_j\}$, $j = 1, \ldots, n$, where $\phi_j > 0 \; \forall j$ and $\sum_j \phi_j = 2\pi$. Due to the symmetry we have

$$p_j = \phi_j/2\pi,$$

and consequently the mean sojourn time in sector j is

$$S_j = p_j A_j = \frac{256}{45\pi^2} \cdot \phi_j.$$

Hence, for the basic case of upper and lower half disk we obtain the mean sojourn time of

$$S_j = 256/45\pi \approx \underline{1.811}.$$

4.4 Unit Disk: circular cell

Consider first a unit disk and a concentric disk with radius r inside it as depicted in Fig. 7. Without loss of generality we consider point $(0, r)$. It is easy to see that in this case the distance to border in directions ϕ and $\phi + \pi$ are given by (see [6])

$$a_1 = \sqrt{1 - r^2 \cos^2 \phi} - r \sin \phi,$$
$$a_2 = \sqrt{1 - r^2 \cos^2 \phi} + r \sin \phi,$$

where ϕ is the angle anti-clockwise away from the tangent at point $(0, r)$. It follows that the flux of arriving
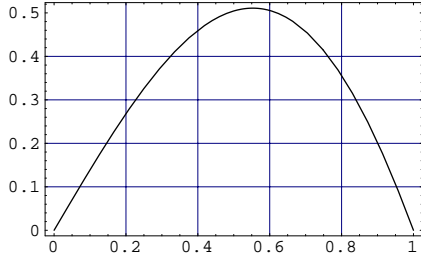
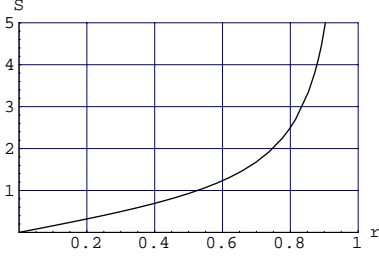Figure 8: The arrival/departure rates to/from a concentric circular cell as a function of the cell radius r.

Figure 9: The mean sojourn time inside a concentric circular cell, $S(r)$, as a function of the cell radius r.

customers into a cell with radius r is,

$$\lambda(r) = \frac{2\pi r}{C_v} \int_0^\pi \sin\phi\,(1-r^2)\sqrt{1-r^2\cos^2\phi}\,d\phi$$

$$= \frac{45\,r(1-r^2)}{64 \cdot \mathrm{E}\,[1/v]} \int_0^\pi \sin\phi\,\sqrt{1-r^2\cos^2\phi}\,d\phi. \quad (21)$$

The mean arrival rate into a concentric circular cell, $\lambda(r)$, is depicted in Fig. 8 as a function of the cell radius r for the case $v = 1$ (constant). It can be seen that the mean arrival rate reaches the maximum, $\lambda \approx 0.511$, at a cell radius of $r \approx 0.553$.

Fig. 9 illustrates the respective mean sojourn time, $S(r)$, which naturally goes to infinity as $r \to 1$. For small values of r we have (cf. Eq. (3))

$$\begin{aligned} p(r) &\approx 2\pi^2 r^2 \cdot h(0)/C &= \pi r^2 \cdot f(0),\\ \lambda(r) &\approx 4\pi r \cdot h(0)/C &= 2r \cdot f(0), \end{aligned}$$

and consequently $S'(0) = \pi/2 \approx 1.571$. Furthermore, $S'(r) > \pi/2 \;\forall\, r > 0$.

4.5 Translated Disk

Consider next a more general case where the disk representing the cell has a different center. In particular, let $\lambda(r, d)$ denote the mean arrival rate into a disk with radius r located d units away from the origin. The situation is illustrated in Fig. 10 with two cells. Cell 1 resides totally inside the RWP domain, while the cell 2 is partly outside the RWP domain. The angle α_0 defines the part of the boundary that must be taken into account in the integration, $\alpha_0, \ldots, \pi$. Similarly as above, starting from Eq. (10)
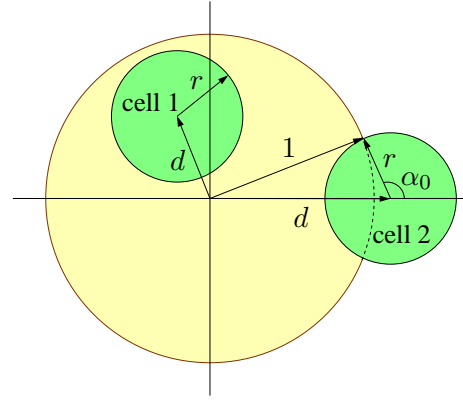

Figure 10: Translated disk cells in unit disk. Cell 1 resides totally inside the RWP domain while cell 2 is only partially reachable by the RWP node(s).

with a little effort one obtains

$$\lambda(r, d) = \frac{2}{C_v} \int_{\alpha_0}^\pi d\alpha\, r(1-x^2) \int_0^\pi d\phi \cdot \\ \sin\phi\sqrt{1-x^2\cos^2(\phi+\alpha-\beta)}, \quad (22)$$

where

$$x^2 = d^2 + 2\,d\,r\cos\alpha + r^2,$$
$$\beta = \arctan(d + r\cos\alpha, r\sin\alpha),$$
$$\alpha_0 = \begin{cases} 0, & \text{when } d+r < 1, \\ \arccos\frac{1-d^2-r^2}{2\,d\,r}, & \text{when } d-r < 1 \le d+r, \\ \pi & \text{otherwise.} \end{cases}$$

For the special case $d = 0$ we have $x = r$, $\alpha_0 = 0$ and $\alpha = \beta$, and, consequently, Eq. (22) reduces to Eq. (21). Furthermore, when velocity is constant $v = 1$, and the radii of the disks are equal, $d = r$, and $r \to \infty$, we obtain the previous example, i.e.

$$\lim_{r\to\infty} \lambda(r, r) = \frac{45\pi}{512}.$$

In Fig. 11 the mean arrival rate into circular cells with different values of the cell (center) distance from the origin is depicted as a function of the cell radius. Obviously, the circular cell having a center at origin obtains the highest mean arrival rate. As the center of the cell moves further way from the origin, the maximum arrival rate is obtained at a larger value of radius r.

Similarly, in Fig. 12 the equivalue contours of the mean arrival rate $\lambda(r, d)$ into a circular cell are depicted. On the x-axis is the radius of the cell r and on the y-axis the distance from the cell center to the origin.

The resulting mean sojourn times for different values of the cell radius r are illustrated in Fig. 13 as a function of the distance between the centers of the disks. For small values of r the mean sojourn time is essentially a constant until the cell moves near the border of the unit disk. Near
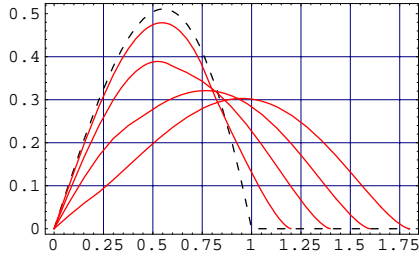
8

Figure 11: Mean arrival rate into a circular cell, $\lambda(r, d)$, as a function of the cell radius r for different values of the cell center distance from the origin $d = 0.0, 0.2, 0.4, 0.6, 0.8$ (from highest to lowest).
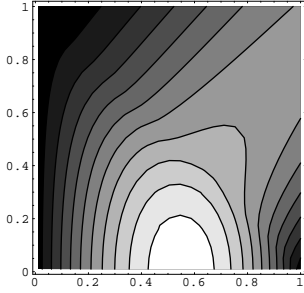

Figure 12: The equivalue contours of the mean arrival rate into a circular cell, $\lambda(r, d)$. On the x-axis is the radius of the cell r and on the y-axis the distance d from the center of the cell to the center of the unit disk.

the border the mean sojourn time first increases due to the fact that most of the visiting nodes make a turn inside the cell instead of passing through it. Then, as d continues to increase and the intersection of the disks becomes smaller the mean sojourn time decreases smoothly to zero.

4.6 Mapping to Pedestrian Model

Suppose that the circular cell in unit disk with radius r corresponds to a cell with a radius of $r^* = 100\,\text{m}$ in a real life scenario. Furthermore, assume that the mobile users move with a constant velocity of $3\,\text{km/h} = \frac{5}{6}\,\text{m/s} \approx 0.83\,\text{m/s}$ (cf. ITU pedestrian model A). Then, using rela-
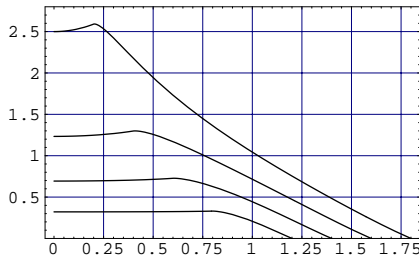

Figure 13: The mean sojourn time inside a circular cell, $S(r, d)$, as a function of the distance from the center of the cell to the origin d for different values of cell radius $r = 0.2, 0.4, 0.6, 0.8$ (from lower to upper).
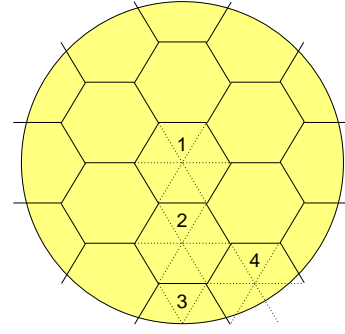

Figure 14: Hexagonal cells: there are 4 different types of cells and 5 different types of handover regions.

tions (19) one obtains $q = 100\,\text{m}/r$ and

$$\frac{S^*}{120\,\text{s}} \cdot r = S(r).$$

As we are interested in the solutions with $0 < r < 1$, we must have $(S'(r) \geq \pi/2)$

$$S^* > 60\pi\,\text{s} \approx 188\,\text{s}.$$

For example, suppose we have measured that a mean sojourn time of a pedestrian mobile user in a cell is $S^* = 4\,\text{min} = 240\,\text{s}$. Substituting that into (19) gives us the corresponding values for our model parameters:

	real-life		model
p^*	$= 0.5878,$	p	$= 0.5878,$
r^*	$= 100\,\text{m},$	r	$= 0.5768,$
λ^*	$= 0.0024492\,\,1/\text{s},$	λ	$= 0.50954,$
S^*	$= 240\,\,\text{s},$	S	$= 1.1536.$

Suppose further, that based on the measurements, we know that the mean number of mobile users in the cell is $n^*_{\text{cell}} = 50$. As the users move independently we have $n^*_{\text{cell}} = m \cdot p^*$, and consequently, in the simulations we should have $m = 85$ mobile users.

4.7 Hexagonal Cellular Network

The last example serves as a more reasonable model for a cellular network. The node is assumed to move with a velocity of 1 in a unit disk. The cellular network consists of 19 cells arranged symmetrically as illustrated in Fig. 14. Due to symmetry we have 4 different cell types and 5 different border segments to be considered. The cell types are indicated in Fig. 14 with numbers $1-4$. Furthermore, we assume that a node moves at a constant velocity of 1.

By numerical calculation we obtain that the arrival rate into the center cell 1 is approximately 0.352. For comparison, the largest disk which fits inside the hexagon cell 1 has a radius of $r_1 = 1/4$, while the smallest disk covering the same hexagon cell has a radius of $r_2 = 1/2\sqrt{3}$. The arrival rates into such circular cells are approximately

	cell 1	cell 2	cell 3	cell 4
area, A_j	0.217	0.217	0.101	0.170
probability, p_j	0.146	0.101	0.011	0.030
arrival rate, λ_j	0.352	0.238	0.039	0.060
sojourn time, S_j	0.414	0.426	0.290	0.494
turns / visit, $N_j^{(T)}$	0.216	0.320	0.917	0.989

Table 2: Results for hexagonal cellular network.

0.326 and 0.367, respectively. The rest of the numerical values are presented in Table 2. Thus, the arrival rate is highest into cell 1 and lowest into cell 3, as the intuition suggests.

The actual handover rates between different cell types are (see Fig. 14)

$$\boldsymbol{\lambda} = \begin{pmatrix} 0 & 0.059 & 0 & 0 \\ 0.059 & 0.049 & 0.022 & 0.030 \\ 0 & 0.022 & 0 & 0.009 \\ 0 & 0.030 & 0.009 & 0 \end{pmatrix}.$$

Note that here we mean by $\lambda_{2,2} = 0.049$ the handover rate from type 2 cell to one of the type 2 neighbouring cells. Hence, the total arrival rate into type 2 cell is

$$\lambda_2 = \lambda_{1,2} + 2 \cdot \lambda_{2,2} + \lambda_{3,2} + 2 \cdot \lambda_{4,2} \approx 0.238.$$

Similarly, the handover rate the mobile node experiences is 2.37 per unit time. For example, if we assume that the unit disk corresponds to a disk with $400\,\mathrm{m}$ radius in real life, and assume that mobile users move at a constant velocity of $3\,\mathrm{km/h}$, then $\overline{v} = 1/480$ and on average 0.59 handovers occur during a typical $2\,\mathrm{min}$ call.

From the table one can also note that the mean sojourn time in different cells varies quite a lot. For example the mean sojourn time in cell 4 is almost twice the mean sojourn time in cell 3. Cells 1 and 2 have equal sizes but are in different locations. The mean sojourn time in cell 2 is somewhat longer than in cell 1. This can be explained by the fact that a node arriving to a cell nearer to the border is more likely to have the next waypoint in the same cell, where as in the case of, e.g., cell 1, a considerable proportion of the arriving nodes pass directly through the cell.

In particular, we note that the mean number of turns per visit, denoted by $N_j^{(T)}$, tends to be strongly dependent on the distance of the cell to the boundary. In the example hexagonal cellular network $N_1^{(T)}$ and $N_2^{(T)}$ are $3-5$ times smaller than $N_3^{(T)}$ and $N_4^{(T)}$. Hence, the visits in the cells 1 and 2 are typically "pass through" type of movement, where as in the cells 3 and 4 the arriving node typically makes one turn before exiting.

4.8 Applicability of the RWP Model

In the RWP model a node takes turns, i.e., changes its direction, on average at the rate of $1/(\overline{\ell} \cdot \mathrm{E}\,[1/v])$ per unit time. Let $f_j^{(T)}$ denote the rate at which turns occur inside a given cell j. As the turning points, i.e., the waypoints, are uniformly distributed over the whole domain $\mathcal{A}$ we have

$$f_j^{(T)} = \frac{A_j}{A \cdot \overline{\ell} \cdot \mathrm{E}\,[1/v]}.$$

Thus, if $f_j^{(T)}$ is much smaller than the arrival rate to cell, λ_j, i.e., if $f_j^{(T)} \ll \lambda_j$, then the majority of the nodes arriving to cell just pass through it and the usability of the RWP model can be argued. In other words, if the area is much larger than the cell, i.e., $A \gg A_j$, then the RWP model hardly characterises the possible intra cell movement.

Also, as mentioned before, in [14] the authors also pointed out that the velocity distribution of the RWP model should be chosen so that the quantity $\mathrm{E}\,[1/v]$ is finite. Otherwise, in the stationary distribution all the nodes are still.

4.9 Composite RWP Mobility Model

As a straightforward extension to overcome the (possible) problem with too straight movement, one could split the area into N overlapping domains denoted by $\mathcal{D}_j$. Then, whenever the waypoint belongs to more than one domain, the node first picks the next target domain among those domains the current waypoint belongs to with some fixed probabilities and then the next waypoint is chosen uniformly from the chosen domain. The conditional pdf of the node location for each domain is still given by (1) with appropriate weights, which are easy to determine by considering the mean rate of turns in each cross section.

This kind of approach could be used to model, e.g., big office buildings, inside a city area. One could, e.g., use a 3-dimensional RWP process to model the mobile users inside the buildings and a 2-dimensional process for the mobile users located outside the buildings. The "exchange" area (cross section) would be located at the bottom of the building.

5 Conclusions

In this paper we have derived analytical formulæ for the mean arrival rate into an arbitrary cell of cellular network when the nodes, i.e., the mobile users, move according to the random waypoint mobility model. The mean handover rate in the network, i.e., the rate at which a mobile node moving according to RWP model makes handovers, is a direct corollary from the mean arrival rates into different cells. Furthermore, the knowledge of the mean arrival rate together with previously known formulæ for the spatial node distribution allow us to derive also the mean sojourn time a cell. For convex cells we were able to derive

the probability that an arriving node has the next waypoint within the cell. This quantity characterises the the frequency of turns along the path from the point of view of a cell. Implications from introducing so-called thinking times at the turning points were also discussed and the corresponding formulæ were presented.

The analytical results were illustrated by several numerical examples and some remarks were made concerning the applicability of the RWP mobility model to the simulation of cellular networks. For simulation purposes the formulæ allow one to adjust other parameters like the shapes and sizes of the cells, mean velocity and the number of nodes, so that the simulation setup matches, as well as possible, with the modelled system.

References

[1] C. Bettstetter, H. Hartenstein, and X. Pérez-Costa. Stochastic properties of the random waypoint mobility model. *ACM/Kluwer Wireless Networks: Special Issue on Modeling and Analysis of Mobile Networks*, 10(5), September 2004.

[2] C. Bettstetter and C. Wagner. The spatial node distribution of the random waypoint mobility model. In *Proceedings of German Workshop on Mobile Ad Hoc networks (WMAN)*, Ulm, Germany, March 2002.

[3] C. Bettstetter. On the connectivity of Ad Hoc networks. *Computer Journal*, 47(4):432–447, July 2004.

[4] C. Bettstetter, G. Resta, and P. Santi. The node distribution of the random waypoint mobility model for wireless ad hoc networks. *IEEE Transactions on Mobile Computing*, 2(3):257–269, July–September 2003.

[5] D. Gross and C.M. Harris. *Fundamentals of Queueing Theory*. John Wiley & Sons, third edition, 1998.

[6] E. Hyytiä, P. Lassila, L. Nieminen, and J. Virtamo. Spatial node distribution in the random waypoint mobility model. Technical Report TD(04)029, COST279, September 2004.

[7] E. Hyytiä and J. Virtamo. Random waypoint model in n-dimensional space. *Operations Research Letters*, 2005.

[8] D.B. Johnson and D.A. Maltz. Dynamic source routing in ad hoc wireless networks. In T. Imielinski and H. Korth, editors, *Mobile Computing*, volume 353, pp. 153–181. Kluwer Academic Publishers, 1996.

[9] P. Lassila, E. Hyytiä, and H. Koskinen. Connectivity properties of random waypoint mobility model for ad hoc networks. In *The Fourth annual Mediterranean workshop on Ad Hoc Networks (Med-Hoc-Net 2005)*, Île de Porquerolles, France, June 2005.

[10] W. Navidi and T. Camp. Stationary distributions for the random waypoint mobility model. *IEEE Transactions on Mobile Computing*, 3(1):99–108, January-March 2004.

[11] J.R. Norris. *Markov Chains*. Cambridge University Press, 1997.

[12] G. Resta and P. Santi. An analysis of the node spatial distribution of the random waypoint model for Ad Hoc networks. In *Proc. ACM Workshop on Principles of Mobile Computing (POMC)*, pp. 44–50, Toulouse, France, October 2002.

[13] Sheldon M. Ross. *Introduction to Probability Models*. Academic Press, 7th edition, 2000.

[14] J. Yoon, M. Liu, and B. Noble. Random waypoint considered harmful. In *Proceedings of Infocom '03*, pp. 1312–1321, San Fransisco, California, USA, April 2003.

Esa Hyytiä received the M.Sc. (Tech.) degree in engineering physics and Lic.Sc. (Tech.) and Dr.Sc. (Tech.) degrees in electrical engineering from the Helsinki University of Technology, in 1998, 2001 and 2004, respectively. His research interests include performance analysis, design and optimization of optical and wireless networks.

Jorma Virtamo received the M.Sc. (Tech.) degree in engineering physics and D.Sc. (Tech.) degree in theoretical physics from the Helsinki University of Technology, in 1970 and 1976, respectively. In 1986, he joined the Technical Research Centre of Finland, VTT Information Technology, where he led a teletraffic research group, and became a Research Professor in 1995. Since 1997 he has been a Professor in the Networking Laboratory of the Helsinki University of Technology. His current research interests include queueing theory and performance analysis and control of the Internet, wireless networks and ad hoc networks.